Photochemical & Photobiological Sciences

PAPER

Effects of gold nanoparticles on the photophysical and photosynthetic parameters of leaves and chloroplasts

Rocio Torres, [ID] [a] Virginia E. Diz [ID] [b] and M. Gabriela Lagorio [ID] *[a,b]

Effects of gold nanoparticles (average diameter: 10–14 nm) on leaves and chloroplasts have been studied. Gold nanoparticles (AuNPs) quenched significantly chlorophyll fluorescence when introduced both in intact leaves and isolated chloroplasts. Additionally, the fluorescence spectra corrected for light re-absorption processes showed a net decrease in the fluorescence ratio calculated as the quotient between the maximum fluorescence at 680 and 735 nm. This fact gave evidence for a reduction in the fluorescence emission of the PSII relative to that of the PSI. Strikingly, the photosynthetic parameters derived from the analysis of the slow phase of Kautsky's kinetics, the rate of oxygen evolution and the rate of photo-reduction of 2,6-dichlorophenolindophenol were increased in the presence of AuNPs indicating an apparent greater photosynthetic capacity. The observed results were consistent with an electron transfer process from the excited PSII, which was thermodynamically possible, and which competed with both the electron transport process that initiated photosynthesis and the deactivation of the excited PSII by fluorescence emission. Additionally, it is here explained, in terms of a completely rational kinetic scheme and their corresponding algebraic expressions, why the photosynthetic parameters and the variable and non-variable fluorescence of chlorophyll are modified in a photosynthetic tissue containing gold nanoparticles.

Introduction

The use of nanoparticles has become increasingly widespread in different areas and applications such as tissue engineering, cancer therapy, manipulation of cells and biomolecules, drug delivery, membrane filtration, additives in toothpaste, pharmaceutical coatings, sunscreen, luminescent biomarkers, biomedical techniques, and alternative energy sources.[1,2]

The extended use foreseen for nanoparticles supposes a greater release to the environment, inevitably leading to the contamination of soil and sub-surface water, a phenomenon that represents a direct influence on plant life. These facts highlight the importance of studying the interaction of these nanomaterials and biota, since due to their nanometric nature, the potential penetration of membranes is very high. Due to the size of the nanoparticles, generally less than 100 nm, they can interact with biomolecules in a complex way.[3] In addition, the nanometric size involves a high contact surface, which modifies reactions that occur on the particles' surface, being able to catalyze certain physiological processes of the plant.[4] In nanoparticulate systems, especially for dimensions of few nanometers, the electronic bands become molecular orbitals which give the material peculiar physical properties.

Gold nanoparticles are outstanding among metal nanoparticulate systems, since they are easy to synthesize, are stable in suspension and have very interesting optical properties which allow nanoparticles to be easily visualized since the light scattered by them is in the visible range.[5–8] In another aspect, they are considered non-toxic nanoparticles.[6,9,10]

In particular, the study of the reciprocal action of nanoparticles in photosynthetic organisms is relevant both in relation to the possible harmful effects on plants (phytotoxicity) and to the possibility of designing hybrid materials with defined properties capable of being used in sensors or other applications.[11] Plasmonic nanoparticles as gold or silver nanoparticles are appealing candidates for this study due to their richness in special optical properties.[12] Moreover, they can easily penetrate leaves through leaf stomata.[13,14] Because of the varied and interesting photophysical and photochemical properties of both these systems (plasmonic nanoparticles and

[a] *CONICET - Universidad de Buenos Aires, Instituto de Química Física de los Materiales, Medio Ambiente y Energía (INQUIMAE), Buenos Aires, Argentina. E-mail: mgl@qi.fcen.uba.ar; Fax: +5411 4576 3341; Tel: +5411 528 58294*
[b] *Universidad de Buenos Aires, Facultad de Ciencias Exactas y Naturales, Departamento de Química Inorgánica, Analítica y Química Física, Buenos Aires, Argentina*

photosynthetic organisms), some types of important interactions including energy and charge transfer processes between nanoparticles and photosynthetic pigments are expected when both are present.

The main photosynthetic pigment in plants is chlorophyll. The spectroscopic and photophysical behavior (especially fluorescence) of chlorophyll-a associated with photosystems I and II has largely been used as a tool for plant health monitoring and to get information about photosynthesis and stress conditions.[15–17] Plant leaves usually display blue, green and red fluorescence. While blue and green emission is due to hydroxycinnamic acids, red emission is caused by the radiative decay of excited chlorophyll-a.[18] More precisely, two peaks are present in the red region: around 685 nm (corresponding to P_{680} in PSII) and around 730 nm (corresponding to both P_{680} in PSII and P_{700} in PSI).[19,20]

Basically there are two ways to study the fluorescence of chlorophyll in plants, either obtaining fluorescence spectra using a steady-state fluorometer, under low illumination conditions so as not to induce variable fluorescence, or by measuring the variable chlorophyll fluorescence as a function of time (Kautsky kinetics).[21,22]

The variable fluorescence of chlorophyll in plants arises from a competition between photosynthesis and light emission processes. In fact, when transferring photosynthetic materials from darkness to light, an increase in the yield of chlorophyll fluorescence is observed. When chlorophyll-a in PSII is excited, it can undergo three competitive deactivation pathways: electron transfer to initiate photosynthesis, heat dissipation or light emission (fluorescence). Once the primary acceptor in the photosynthetic chain has received an electron, it is not able to accept another until the electron has been transferred to the next acceptor. During this time (about 1 second), the reaction center is said to be closed and the fluorescence emission increases. Afterwards, fluorescence starts to fall within a period of several minutes to reach a stationary state.[22]

The interaction of gold nanoparticles (AuNPs) with chlorophyll has already been studied by several authors. Barazzouk et al. proved that AuNPs quenched chlorophyll-a fluorescence, in solution, due to photoinduced electron transfer from the excited photosynthetic pigment to the nanoparticles.[23] Later, this research group used AuNPs, in micromolar concentration, to photoprotect chlorophyll-a in solution.[24] They found that AuNPs were more protective than natural plant photo-protectors such as beta carotenes or quinones. In their work, they proposed a binding between AuNPs and the N atoms of chlorophyll-a, which avoided their degradation by reactive oxygen species.

In vivo observation of chlorophyll fluorescence quenching, induced by gold nanoparticles, was also reported by Falco et al. who treated soybean seeds and leaves at surface level with AuNPs.[25]

Recently, Giraldo et al. have published some fascinating results on the promotion of the photosynthetic activity in plant organelles containing single-walled carbon nanotubes. They also reported that the nanotubes enabled NIR fluo-
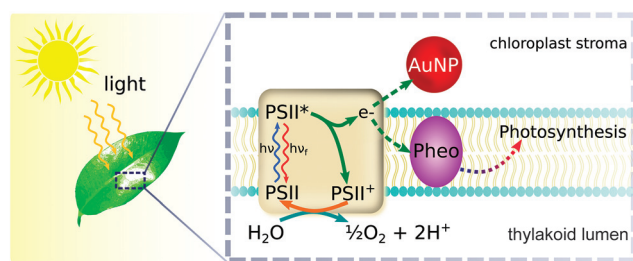

Fig. 1 A schematic diagram of the photophysical and photochemical processes studied for the system AuNPs–photosynthetic material.

rescence monitoring of nitric oxide in vivo, suggesting the use of the hybrid system as a photonic chemical sensor.[26]

Although chlorophyll fluorescence quenching by AuNPs has already been reported in plants, a comprehensive spectroscopic study is lacking at both leaf and chloroplast-levels. Even more, developing a detailed mechanism of the photophysical processes that take place in the AuNP–plant system is relevant for the correct interpretation of the photosynthetic parameters, such as the quantum yield of photosystem II and non-photochemical quenching among others, usually obtained from the variable chlorophyll fluorescence.

Taking into account these vacancies in the literature, the goal of this work was to study comparatively the effect of the AuNPs in leaves and chloroplasts on the absorption of light, on the variable and non-variable fluorescence of chlorophyll and on photosynthesis, rationalizing the results by means of a detailed kinetic mechanism and their respective algebraic equations. The photophysical and photochemical processes outlined schematically in Fig. 1 are addressed in this work.

Since the processes of light re-absorption in the plant leaves can noticeably alter the observed results, they were thoroughly taken into account in the whole analysis by application of physical models previously developed.[21] To the best of our knowledge, this is the first time that these correction models are used for the proper interpretation of the optical signals originating from this hybrid system: AuNPs–photosynthetic material.

All these aspects are important in the context of being able to give a detailed description of what happens in the system and how the photochemical processes of the plant can be affected by the AuNPs.

Materials and methods

Synthesis and characterization of gold nanoparticles

Gold nanoparticles (AuNPs) were synthesized according to the literature.[27] Briefly, a solution of water (20 mL) containing 4 mL of 1% sodium citrate and 0.05 mL of 1% tannic acid was heated to 60 °C and added under stirring to a solution of 0.25 mM tetrachloroauric acid (1 mL) in Milli-Q water (80 mL) kept at 60 °C. As soon as a ruby-red color solution was obtained, the reaction mixture was maintained at 60 °C under

506 | Photochem. Photobiol. Sci., 2018, 17, 505–516

This journal is © The Royal Society of Chemistry and Owner Societies 2018

stirring for 10 more minutes. The resultant suspension contained AuNPs in the synthesis medium at pH = 5.

A solution of sodium citrate (1 mM) and tannic acid (3 μM), with pH = 5, which was analogous to the medium in which the gold nanoparticles were dispersed, was used as the control solution.

The particles obtained were characterized by scanning and transmission electron microscopy, which are described in greater detail below, UV-VIS spectroscopy, dynamic light scattering (DLS) and zeta potentials.

The absorbance spectra were recorded on a UV-VIS-NIR spectrophotometer (Shimadzu UV-3600 Plus) with quartz cuvettes. The hydrodynamic diameter and the zeta potential of the particles were measured using a DLS 90 Plus/BI-MAS (Brookhaven Instrument Co, EE.UU.), equipped with a He–Ne laser operating at 632.8 nm and a zeta-potential analyzer (Brookhaven Instrument Corp, EE.UU).

Inoculation of leaves and chloroplasts with AuNPs

The plant species used in this study was *Robinia pseudoacacia* L. Leaves of similar size and structure were obtained from a nearby tree and washed for immediate use with Milli-Q water. The leaves were then arranged individually in plastic containers. Half of the leaves were completely covered with control solution and the other half with the solution containing AuNPs. They were illuminated with artificial white light using a Philips 7748SEHJ lamp (24 V–250 W). The lighting was carried out for two hours before the measurements in order to open the stomata and to allow the incorporation of the AuNPs. Each batch of samples consisted of six control leaves and six hybrid systems (AuNPs–leaf).

On each leaf, measurements of transmittance, reflectance, initial fluorescence and variable fluorescence (Kautsky kinetics) were recorded on the same day (see the section Spectroscopic and photophysical analysis below). These measurements were performed 5, 24, 48, 72 and 86 hours after the immersion of the leaves in the nanoparticle suspension or in the control solution.

Isolated chloroplasts were obtained from the leaves of *Robinia pseudoacacia* L. using differential centrifugation, following the literature.[28,29] Then, chloroplasts were suspended, under cooling conditions, in a suspension medium (SM) composed of 0.5 M sucrose, 50 mM Tris-HCl, pH 7.5, 20 mM KCl, 5 mM $MgCl_2$, 1 mM $MnCl_2$ and 2 mM EDTA. Finally, sucrose gradients were used to obtain chloroplasts whose membrane remained intact. Chloroplasts were stored at −10 °C after isolation for not more than 48 hours.

In particular, for the oxygen evolution rate studies (see the section Oxygen evolution rate measurements), the medium additionally contained $NaHCO_3$ (10 mM).

A buffer solution analogous to SM but containing gold nanoparticles was prepared. Thus, we worked with chloroplast suspensions of both control chloroplasts and AuNPs-chloroplasts in the same medium buffer. On these suspensions, photophysical studies, Hill reaction and analysis of oxygen evolution under saturating light conditions were performed.

Spectroscopic and photophysical analysis

Reflectance and transmittance. Diffuse reflectance (R) and diffuse transmittance (T) spectra of leaves were recorded on a Shimadzu 3101PC spectrophotometer equipped with an integrating sphere. Barium sulphate was used as a standard to adjust the 100% reflectance level. Measurements between 300 and 2500 nm were recorded. From these data, the remission function, $F(R)$, a quantity proportional to chromophore concentration, was calculated as $(1 − R)^2/(2R)$.[21,30]

Non-variable fluorescence. Emission spectra of dark-adapted intact plant leaves were obtained under low photon flux excitation (20 μmol m^{-2} s^{-1}). Under these conditions, the so called initial fluorescence F_0 was recorded as a function of wavelength. Measurements were carried out on a Quanta Master 400 steady-state spectrofluorometer (Photon Technology Inc., London, Ontario, Canada) using a front-face geometry with an angle of 60°. Prior to measurements, plants were dark-adapted for 15 min.

Due to the overlap of the absorption and emission spectra of the leaves (see Fig. 4), there was an artifact in the experimental fluorescence spectra that enhanced the band at 735 nm compared to the band at shorter wavelength, due to light re-absorption processes.[21] As a consequence, emission spectra were distorted and the peak ratio was underestimated. To eliminate light reabsorption artifacts, thick layer fluorescence spectra were corrected for reabsorption according to Ramos and Lagorio.[30] True emission spectra were obtained using this method developed by our working group and this method has been successfully applied to correct fluorescence spectra of leaves and fruits.[21,30–32]

For chloroplast fluorescence measurements, a thin layer of chloroplasts was deposited on a glass slide. To achieve this, the chloroplast suspension was centrifuged and a portion of the sediment was taken and spread using a spatula on a glass slide. The water contained in the deposited material was then allowed to evaporate at room temperature until the chloroplasts remained adhered to the glass support. The layers were prepared with decreasing thickness and the emission spectra were recorded until no changes in the ratio of fluorescence maxima (680 and 735 nm) were obtained. The final fluorescence spectra so obtained were taken into account and they were considered free of light re-absorption processes.[30]

The emission spectra for leaves or chloroplasts were obtained from 600 to 800 nm at two different excitation wavelengths (460 and 520 nm) and corrected by an instrumental factor (included in the fluorometer software), which took into account the response of the detector to different wavelengths. The fluorescence spectra were recorded as the number of photons emitted as a function of wavelength. The low photon flux used (lower than 20 μmol m^{-2} s^{-1}) ensured the non-induction of fluorescence kinetics. Under these conditions, all electron receptors were open and the measured fluorescence was very close to the emission of the ground state (F_0). The excitation wavelength corresponding to 460 nm led to the highest fluorescence signal, while the excitation at 520 nm corre-

This journal is © The Royal Society of Chemistry and Owner Societies 2018

Photochem. Photobiol. Sci., 2018, **17**, 505–516 | 507

sponded to the maximum absorption of the plasmon of the gold nanoparticles (see Fig. 2).

Variable chlorophyll fluorescence: Kautsky kinetics. Variable chlorophyll fluorescence (Kautsky kinetics) was investigated using a pulse-modulated chlorophyll fluorometer (PAM Hansatech FMS1), on leaves that had been previously dark-adapted for 15 min. For excitation, a 594 nm amber modulating beam, which induced a pulse fluorescence signal under conditions where ambient light was excluded, was used. The pulse duration of the modulating beam was short with long off periods between pulses. The incident radiation upon the sample coming from the modulating beam was lower than 0.05 μmol m^{-2} s^{-1} as to avoid significant physiological changes in the sample. The saturating pulse (halogen light) was set to 14 400 μmol m^{-2} s^{-1} with a duration of 0.4 s. The actinic light was provided by a halogen light source of about 600 μmol m^{-2} s^{-1}. The sampling rate was automatically varied from 10 Hz to 20 kHz (low frequency for F_0 measurement and high frequency during application of actinic or saturating light). The experiments were started recording the minimum fluorescence signal from dark-adapted samples (F_0) with the modulating beam. Then the saturating pulse was applied and the maximum fluorescence F_m was recorded allowing calculation of F_v/F_m ($F_v = F_m - F_0$). Afterwards, the samples were exposed to the actinic light for several minutes. After this time period, a steady state fluorescence value F_s was reached, and a new saturating pulse was applied to record the maximum fluorescence for light-adapted leaves (F'_m). Another saturating pulse was applied, the actinic light was turned-off and the far-red pulse was applied for F'_0 determination. From these data, the maximum quantum efficiency of PSII photochemistry (F_v/F_m) and the quantum efficiency of PSII ($\Phi_{PSII} = (F'_m - F_s)/F'_m$) were calculated, among other parameters.[22,32]
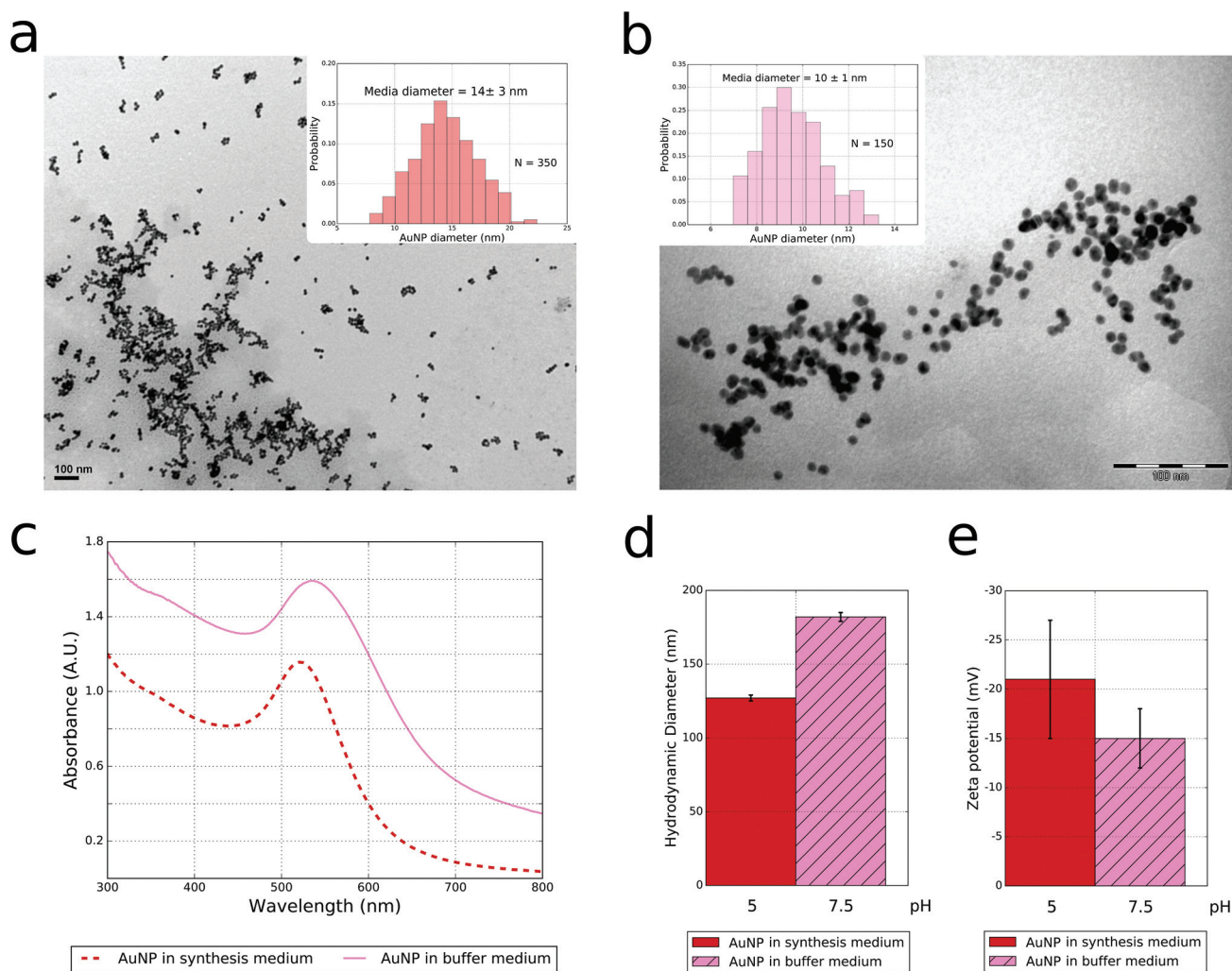

Fig. 2 Characterization of AuNPs in the synthesis medium and in the chloroplast suspension buffer (pH = 7.5). (a) Transmission electron microscopy (TEM) of AuNPs in the synthesis medium (magnification 100 000) and its corresponding size distribution histogram in the inset. (b) TEM of AuNPs in the chloroplast suspension buffer (magnification 140 000) and its corresponding size distribution histogram in the inset. (c) Absorbance spectra of AuNPs, (d) hydrodynamic diameter for AuNPs and (e) the Z potential of AuNPs.

508 | *Photochem. Photobiol. Sci.*, 2018, **17**, 505–516

This journal is © The Royal Society of Chemistry and Owner Societies 2018

Scanning and transmittance electron microscopy (SEM and TEM)

The samples were mounted on pieces of silica with double-sided tape. The assembled samples were observed at 20 kV under a scanning electron microscope, Zeiss SUPRA 40. The micrographs were obtained using a coupled CCD camera.

Drops of the nanoparticle suspension were examined by using a TEM microscope (JEM 1200EX II).

Subsequently, the incorporation of AuNPs into chloroplasts was confirmed by TEM images (results not shown). In this last case, uranyl acetate was used as a negative contrast agent and a Philips EM300 transmission electron microscope was used.

Hill reaction

The Hill reaction was studied in order to obtain information about the photosynthetic activity of chloroplasts under the influence of added nanoparticles. This reaction was so performed on chloroplast suspensions (control and AuNP-inoculated) according to the literature.[33,34] The probe DCPIP (2,6-dichlorophenolindophenol) was used as an acceptor of the electrons flowing from PSII to PSI under illumination. This dye, which acted as a sensor of the electron transport in the photosynthetic chain, changed its color from blue to colorless as photosynthesis proceeded. The color change was quantified by measuring absorbance at 607 nm and using an extinction coefficient of 20 mM^{-1} cm^{-1} for DCPIP. A halogen lamp of 75 W (Osram) coupled with a water filter that absorbed mainly in the region of the IR produced cold white light which was used to induce the reduction of DCPIP (in the presence of photosynthetic materials) under the conditions of non-saturation. The chlorophyll concentration in each tested suspension was on average 0.3 mg ml^{-1} and the concentration for DCPIP was approximately 1 mM. The visible absorption spectra were recorded using a Shimadzu UV-3600 spectrophotometer with disposable 1 cm optical cells. The illumination was applied in total for 5 minutes, recording the absorbance spectra every 15 seconds during the first 1.5 minutes of illumination, then every 30 seconds for the next 1.5 minutes of irradiation and every 1 minute, for the remaining 2 minutes. Additionally, the decomposition of DCPIP was tested both for a blank containing only AuNPs (3 ppm) and the DCPIP probe (without chloroplasts), in the dark and with illumination, and for suspensions of chloroplasts (or chloroplasts-AuNPs) with DCPIP, kept in the dark.

Oxygen evolution rate measurements

Oxygen evolution for chloroplast suspensions (both control and AuNP-inoculated) was measured polarographically using an aqueous phase Clark-type oxygen electrode (Hanna Instruments HI 9146) following the literature.[29,35,36] Measurements were performed using a 18 ml reaction mixture containing 50 mM Tricine-HCl buffer (pH 7.4), 0.5 M sucrose, 20 mM KCl, 5 mM MgCl$_2$, 10 mM NaHCO$_3$, 30 μM DCPIP as the artificial electron acceptor and a volume of chloroplast preparation containing 80–100 μg ml^{-1} of chlorophyll. The reactions were run at 20 °C and actinic light was supplied using a 75 W halogen lamp coupled with a water filter.

Chlorophyll concentration in chloroplasts

The total concentration of chlorophyll in the chloroplast preparation was measured according to Sims and Gamon,[37] and rapid calculations according to Porra *et al.*[38]

The whole set of experiments was carried out at room temperature.

Results and discussion

Characterization of gold nanoparticles

TEM images of AuNPs suspended both in the synthesis medium (pH = 5.0) and in the buffer used for chloroplast resuspension (pH = 7.5) are shown in Fig. 2a and b, respectively. Their respective histograms for dry diameters are presented as insets in the same figures, showing mean diameters of 14 ± 3 nm and 10 ± 1 nm, respectively. No significant differences were found between the mean nanoparticle diameters in both media and both populations of particles presented a unimodal distribution.

AuNP hydrodynamic diameters obtained by DLS were 127 ± 2 nm in the synthesis medium and 182 ± 3 nm in the buffer suspension (Fig. 2d). Their zeta potentials were negative for both media indicating a negative surface charge. The value for AuNPs in the synthesis medium was −21 ± 6 mV and −15 ± 3 mV in the buffer suspension (Fig. 2e). The Z potential values were comparable to those in the literature.[39,40] The absorbance spectra of AuNPs exhibited accordingly the typical plasmon absorption maximum at 520 ± 3 nm (Fig. 2c).

The results indicate that the AuNP size was not substantially altered when they were transferred from the synthesis medium to the buffer solution. However, the presence of a greater amount of ions in the buffer solution with respect to the synthesis medium caused a decrease in the absolute surface charge of the colloid (less negative) as previously published in the literature.[41]

The plasmon absorption at about 520 nm was consistent with a mean AuNP diameter of around 10 nm.[42,43] It is well known that a higher ionic strength usually increases nanoparticle attraction, so it is common to find nanoparticle aggregation in media with greater ion concentration.[44] Differing from the dry diameter, the hydrodynamic diameter augmented in the buffer solution accordingly with the slight shift in the absorbance spectrum. A slight widening of the band is also observed in the case of the buffer medium, which is indicative of a less homogeneous size distribution.

Spectroscopy and photophysical analysis

Spectroscopy of leaves, chloroplasts and AuNPs. In Fig. 3, the typical reflectance spectra for leaves are shown. Upon inoculation with AuNPs, changes took place both in the NIR and in the visible part of the spectrum. The most evident vari-
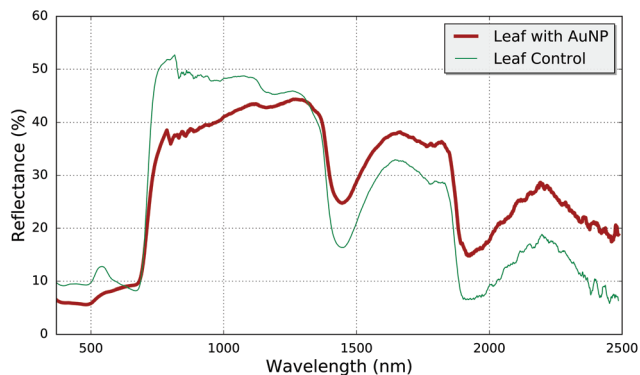
This journal is © The Royal Society of Chemistry and Owner Societies 2018

Photochem. Photobiol. Sci., 2018, **17**, 505–516 | 509

Fig. 3 Typical reflectance spectra obtained for leaves of *Robinia pseudoacacia* in the presence and absence of AuNPs in the region of the visible (left) and in the near infrared (right).

Fig. 4 Normalized absorbance and emission spectra of chloroplasts and normalized absorbance of gold nanoparticles (AuNPs) in the buffer medium.

ation was a decrease in the reflectance jump between the red and far-red regions.

In the visible region (400–700 nm), reflectance spectra of leaves are mainly determined by the light absorption of leaf pigments. In particular, the sharp change in reflectance between 650 and 700 nm is related to chlorophyll content and early stress. On the other hand, in the near infrared region, leaf reflectance is influenced by cell structure (740–1350 nm) and by water content (1350–2500 nm). The observed variations of the reflectance spectrum in the NIR region would indicate a slight decrease in water content and alteration of the cellular structure when AuNPs are present. Additionally, the reduction of reflectance values in the visible region is due to the presence of AuNPs that add their own absorption of light to that of photosynthetic pigments. Finally, the reduction in the reflectance jump in the red edge (650–700 nm) for leaves with AuNPs is a clear sign of stress.

Chloroplast suspension strongly absorbed between 400 and 500 nm and between 650 and 700 nm, while AuNPs displayed their plasmon absorption around 520 nm typical of gold nanoparticle sizes about tens of nanometer. Fig. 4 shows these absorption spectra together with the emission fluorescence spectra of chloroplasts in the red and far-red regions. An important overlap between the absorption and the emission spectra of chloroplasts can be clearly seen in the figure, especially for the emission band in the red region (around 680 nm).

Non-variable chlorophyll fluorescence. Fluorescence spectra for the initial (non-variable) fluorescence both for leaves and chloroplasts in the presence or absence of nanoparticles are presented in Fig. 5. Specifically, experimental spectra for leaves are shown in Fig. 5a and experimental spectra for chloroplast suspension in Fig. 5b. The leaf spectra additionally corrected by light re-absorption, in order to discard artifacts due to differences in pigment concentration and reflectance, were obtained and the resultant fluorescence ratios, calculated as the quotient between the maximum fluorescence at 680 and 735 nm, are displayed in Fig. 5c, where the error bars correspond to the standard deviation calculated after averaging the fluorescence ratios.
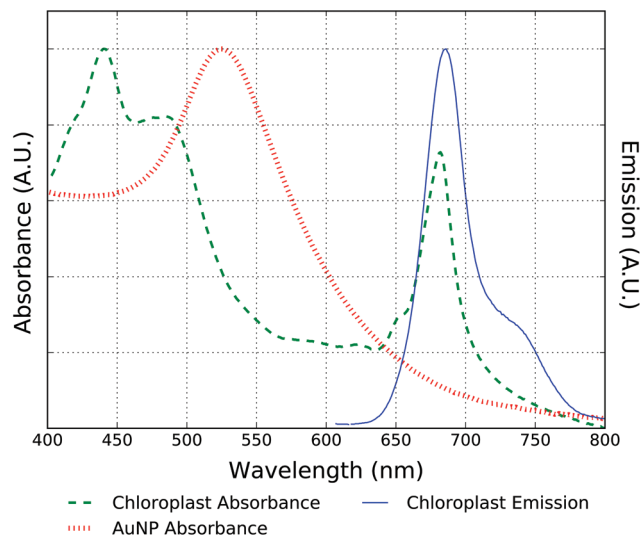
The spectra shown in Fig. 5a are affected by various processes, such as the light filter due to AuNPs and the reabsorption of fluorescence, which complicates the direct interpretation and comparison of these spectra. Nevertheless, it should be noted that the ratios of fluorescence intensities in the red and far red regions (calculated on the spectra corrected by reabsorption) are independent of the aforementioned factors (Fig. 5c).

The correction for light re-absorption processes was performed only for the fluorescence spectra of leaves. It was not necessary for isolated chloroplasts, where it was assumed that these artifacts were absent.[30] For leaves with AuNPs, the data shown correspond to 86 hours of immersion (during the immersion time it was observed that the changes became more accentuated following a definite trend). Several important facts arise from these results. First, a net quenching of chlorophyll fluorescence due to the presence of AuNPs was observed both in leaves and isolated chloroplasts. Secondly, AuNPs induced a decrease in the fluorescence ratio ($F_{red}/F_{far-red}$) corrected by light re-absorption processes. In fact, for leaves excited at 460 nm, the corrected fluorescence ratio decreased from 2.72 ± 0.09 (control) to 1.86 ± 0.06 (AuNPs inoculated) while for chloroplasts from 2.85 ± 0.51 to 1.84 ± 0.17. Additionally, mean values for the fluorescence ratio of leaves corrected by light re-absorption agreed with mean values for this ratio in chloroplasts.

It should be noted that the fluorescence ratio observed from an intact leaf is strongly affected by fluorescence re-absorption due to the high pigment concentration in plants and the important overlap between absorption and fluorescence spectra (Fig. 4). Thus, the most affected band is placed in the red region (680 nm).

The fluorescence ratio connected with the physiological state of the plant is not the experimental one emerging from a
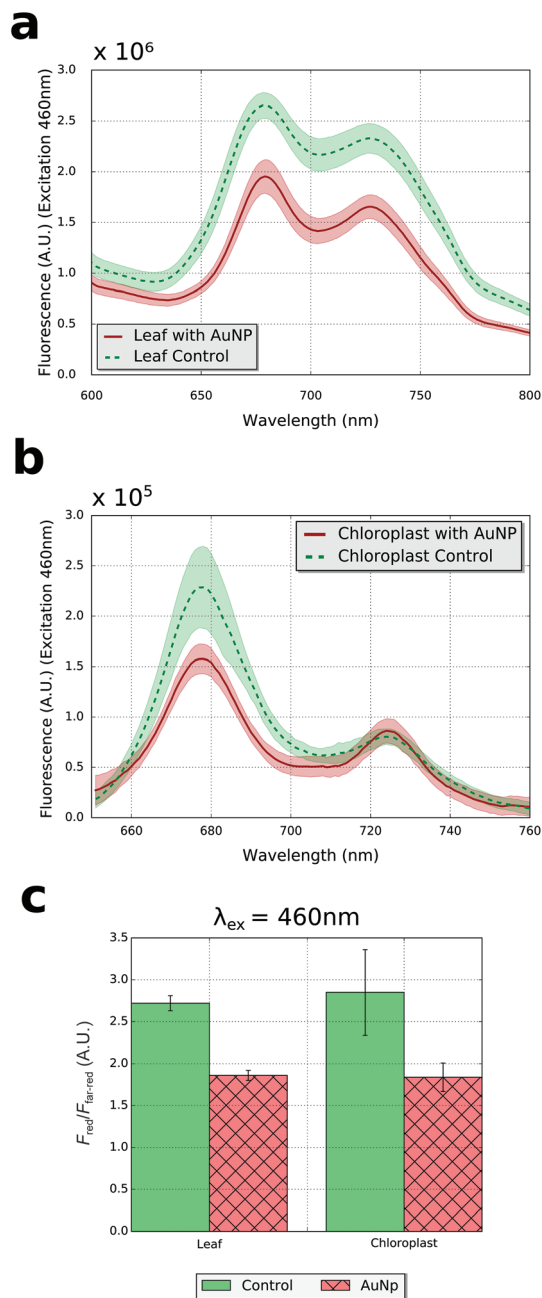
510 | *Photochem. Photobiol. Sci.*, 2018, **17**, 505–516

This journal is © The Royal Society of Chemistry and Owner Societies 2018

Fig. 5 Initial non-variable fluorescence (F_0) for leaves and chloroplasts (in the presence or absence of AuNPs). (a) Experimental F_0 spectra for leaves previously adapted to darkness (excitation wavelength: 460 nm) corrected for the detector response. (b) Experimental F_0 spectra for isolated chloroplasts (excitation wavelength: 460 nm) corrected for the detector response. (c) The fluorescence ratio ($F_{red}/F_{far-red}$) for leaves (corrected for light re-absorption processes) and for isolated chloroplasts at an excitation wavelength of 460 nm. The shaded areas in (a and b) and the error bars in (c) indicate the standard error of the measurements.

leaf but that emerging from a chloroplast (that agrees with the ratio from a leaf corrected by the artifacts). Therefore, the correction by re-absorption of the fluorescence is extremely relevant.

Excitation at the nanoparticle plasmon (520 nm) also led to a decrease in the fluorescence ratio when AuNPs were present (results not shown).

Variable chlorophyll fluorescence: Kautsky kinetics. Typical records of Kautsky kinetics obtained for control leaves and leaves inoculated with AuNPs are shown in Fig. 6. The resultant fluorescence and photosynthetic parameters are displayed in Fig. 6. The initial (F_0) and maximum (F_m) fluorescence observed in the presence of nanoparticles were lower than for the control, which agreed with the fluorescence quenching effect of AuNPs observed in the measurements of non-variable chlorophyll fluorescence.

At the excitation wavelength of the PAM fluorometer (see the section Variable chlorophyll fluorescence in Materials and methods), both the AuNPs and the P_{680} of PSII could be excited. Absorption of light by AuNPs could lead to energy transfer to P_{680} in PSII (see Fig. 4 to compare absorption maxima). However, as this process would lead to an enhancement of chlorophyll fluorescence that is not observed, we considered negligible the rate of energy transfer. On the other hand, if AuNPs absorbed light and did not transfer energy, they would act by adding an internal filter effect.

In the literature, there are several studies where the quenching of chlorophyll-a fluorescence in solution has been reported. This quenching was generally attributed to electron transfer from the excited singlet of chlorophyll-a to different acceptors.[45–49] In particular, Barazzouk et al. found photoinduced electron transfer between chlorophyll-a and gold nanoparticles.[23] In fact, they demonstrated that excited chlorophyll-a donated an electron to gold nanoparticles, a process that was thermodynamically feasible since the reduction potential for excited chlorophyll-a is −1.1 V vs. the NHE and the Fermi level of Au^0 is +0.5 V vs. the NHE according to these authors.
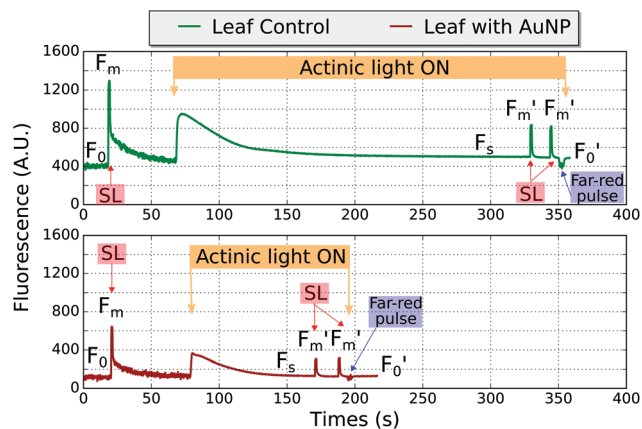

Fig. 6 Typical records of the variable chlorophyll fluorescence recorded with a pulse-modulated fluorometer for leaves inoculated with control solution and leaves inoculated with AuNP suspension. The leaves were previously dark-adapted for 15 min. "SL" indicates a saturating light pulse.
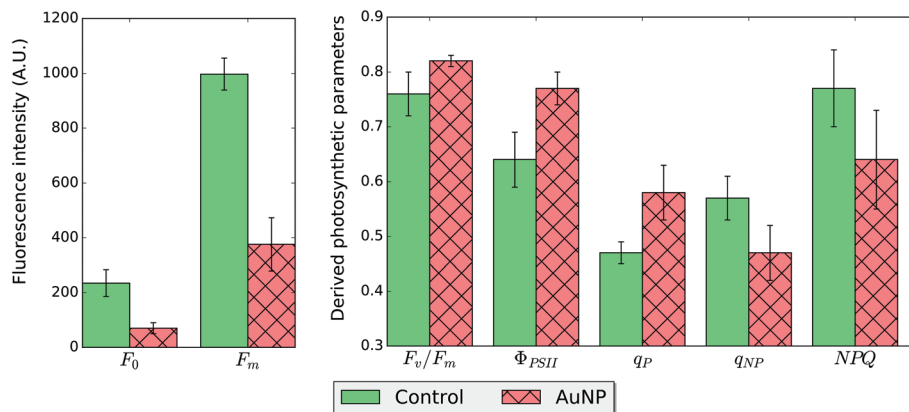
This journal is © The Royal Society of Chemistry and Owner Societies 2018

Photochem. Photobiol. Sci., 2018, 17, 505–516 | 511

Fig. 7 Variable fluorescence parameters for leaves in the presence and absence of AuNPs.

In the present work, with photosynthetic materials, we have also detected chlorophyll-a fluorescence quenching (Fig. 5–7) and taking into account the value around -0.62 to -0.66 V for the reduction potential of the excited state of P_{680} in PSII ($E^{\circ}P_{680}{}^{+}/P_{680}^{*}$ *vs.* the NHE according to Kato *et al.* or -0.7 V according to Merchant *et al.*), the photoinduced electron transfer to AuNPs, with a Fermi level $\sim +0.7$ V to $+0.5$ V (for AuNPs of similar size as reported by Barazzouk *et al.*), is still thermodynamically favorable.[23,50–52] Thus, taking into account the experimental data and the previous studies in the literature, only light absorption, charge transfer processes and inner filter effects were considered for AuNPs.

The parameters corresponding to the dark-adapted state are ground Chl fluorescence (F_0), maximum Chl fluorescence induced by a saturating pulse (F_m) and the maximum quantum yield of PSII (F_v/F_m). The parameters corresponding to the light-adapted state are the quantum yield of PSII (Φ_{PSII}), photochemical quenching (q_p) and non-photochemical quenching (q_{Np}) of variable Chl fluorescence, and non-photochemical quenching (NPQ). All data represent the means ± S.E. (from at least six independent series of experiments).
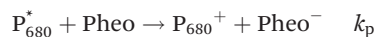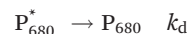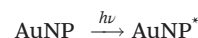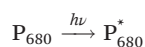
From the analysis of the Kautsky kinetics (Fig. 7), it resulted that:

• F_0, F_s and F_m were significantly lower in the presence of AuNPs.

• F_v/F_m was significantly higher in the presence of AuNPs.

• The quantum yield of PSII and q_P were significantly higher in the presence of AuNPs.

• q_{NP} and NPQ were significantly lower in the presence of AuNPs.

All data were tested using ANOVA, with $p < 0.05$.

To rationalize the meaning of these photophysical parameters when AuNPs are present, it is convenient to solve a general kinetic scheme, where the charge transfer process was introduced in parallel with the photosynthetic processes and other photophysical decays:

$$P_{680} \xrightarrow{h\nu} P_{680}^{*}$$

$$AuNP \xrightarrow{h\nu} AuNP^{*}$$

$$P_{680}^{*} \rightarrow P_{680} \quad k_d$$

$$P_{680}^{*} \rightarrow P_{680} + h\nu_f \quad k_f$$

$$P_{680}^{*} + Pheo \rightarrow P_{680}{}^{+} + Pheo^{-} \quad k_p$$

$$P_{680}^{*} + AuNP \rightarrow P_{680}{}^{+} + (AuNP)^{-} \quad k_{ct}$$

with $k_d + k_f = k_c$.

In this scheme, k_c represents the rate constant for the photophysical decay of P_{680}^{*}, k_p the rate constant for the primary step of the photosynthesis process and k_{ct} the rate constant for the electron transfer from P_{680}^{*} to AuNPs.

From this general mechanism, the different photosynthetic parameters can be expressed in terms of the rate constants.[53]

F_0 may then be written by eqn (1) and (2) in the absence or presence of AuNPs, respectively.

$$F_0 = G \frac{k_f}{k_c + k_p} \tag{1}$$

$$F_0^{AuNP} = G' \frac{k_f}{k_c + k_{ct} + k_p}, \tag{2}$$

with $G' < G$, where G is an instrumental factor. The inner effect of AuNPs has been qualitatively included in G' stating that G' is lower than G. Assuming the same values for k_f, k_c and k_p for both situations, it may be seen that a lower value for F_0 is predicted in the presence of AuNPs due to the charge transfer process and inner filter.

Analogously, a decrease in F_s^{AuNP} compared to F_s is predicted from eqn (3) and (4):

$$F_s = G \frac{k_f}{k_c + k_{NPQ} + k_p} \tag{3}$$

$$F_s^{AuNP} = G' \frac{k_f}{k_c + k_{NPQ} + k_{ct} + k_p}. \tag{4}$$

512 | *Photochem. Photobiol. Sci.*, 2018, **17**, 505–516

This journal is © The Royal Society of Chemistry and Owner Societies 2018

When a saturating pulse is applied, no charge transfer is possible (neither the photosynthetic process nor the charge transfer to AuNPs) due to the fact that all electron acceptors are reduced and a maximum value of F_m is obtained. At this point, the equations for F_m are

$$F_m = G \frac{k_f}{k_c} \tag{5}$$

$$F_m^{AuNP} = G' \frac{k_f}{k_c}, \tag{6}$$

and the lower value for G' compared to G would explain the experimental result $F_m^{AuNP} < F_m$.

For the maximum quantum yield (F_v/F_m), it is described by eqn (7) and (8) in the absence or presence of AuNPs, respectively:

$$\frac{F_v}{F_m} = \frac{F_m - F_0}{F_m} = \left(\frac{k_f}{k_c} - \frac{k_f}{k_c + k_p}\right)\frac{k_c}{k_f} = \frac{k_p}{k_c + k_p} \tag{7}$$

$$\left(\frac{F_v}{F_m}\right)^{AuNP} = \frac{F_m - F_0}{F_m} = \left(\frac{k_f}{k_c} - \frac{k_f}{k_c + k_{ct} + k_p}\right)$$
$$\frac{k_c}{k_f} = \frac{k_{ct} + k_p}{k_c + k_{ct} + k_p}. \tag{8}$$

Experimentally, it was found that

$$\frac{F_v}{F_m} < \left(\frac{F_v}{F_m}\right)^{AuNP}. \tag{9}$$

This inequality may be written in terms of the rate constants as

$$\frac{k_p}{k_c + k_p} < \frac{k_{ct} + k_p}{k_c + k_{ct} + k_p} \rightarrow \frac{k_c + k_{ct} + k_p}{k_c + k_p}$$
$$< \frac{k_{ct} + k_p}{k_p} \rightarrow \frac{k_{ct}}{k_c + k_p} < \frac{k_{ct}}{k_p} \tag{10}$$
$$\rightarrow k_c + k_p > k_p \rightarrow k_c > 0,$$

which due to the positive values for the rate constants is always fulfilled. This shows that even when there is not an actual increment in photosynthesis the occurrence of the charge transfer process towards the nanoparticles causes an apparent false increase in the maximum quantum yield of photosynthesis. In other words, in the presence of AuNPs F_v/F_m no longer represents the yield of photosynthesis but the performance of the sum of the two processes of electron transfer: photosynthesis and charge transfer to the nanoparticles.

A similar scenario is found for the quantum efficiency of PSII given by eqn (11) and (12):

$$\Phi_{PSII} = \frac{F'_m - F_s}{F'_m} = \frac{k_p}{k_c + k_{NPQ} + k_p} \tag{11}$$

$$(\Phi_{PSII})^{AuNP} = \frac{F'_m - F_s}{F'_m} = \frac{k_{ct} + k_p}{k_c + k_{NPQ} + k_{ct} + k_p}. \tag{12}$$

Experimentally (see Fig. 7)

$$\Phi_{PSII} < (\Phi_{PSII})^{AuNP}. \tag{13}$$

In terms of the rate constants, the inequality (13) is given by eqn (14)

$$\frac{k_p}{k_c + k_{NPQ} + k_p} < \frac{k_{ct} + k_p}{k_c + k_{NPQ} + k_{ct} + k_p}$$
$$\rightarrow \frac{k_c + k_{NPQ} + k_{ct} + k_p}{k_c + k_{NPQ} + k_p} < \frac{k_{ct} + k_p}{k_p} \tag{14}$$
$$\rightarrow \frac{k_{ct}}{k_c + k_{NPQ} + k_p} < \frac{k_{ct}}{k_p} \rightarrow k_c + k_{NPQ} + k_p$$
$$> k_p \rightarrow k_c + k_{NPQ} > 0,$$

which is always valid due to the positive values for the rate constants.

As in the case of F_v/F_m the increase in PSII efficiency observed with AuNPs is erroneous and false. What is calculated under these conditions is not Φ_{PSII} but the quantum efficiency for the two processes that involve electron transfer from P^*_{680} together.

For the non-photochemical quenching q_{NP}, the experimental result is

$$q_{NP} > q_{NP}^{AuNP} \tag{15}$$

Here again the occurrence of the charge transfer process to AuNPs distorts the meaning of this parameter. In fact considering that

$$F'_m = G \frac{k_f}{k_c + k_{NPQ}} \tag{16}$$

$$F'^{AuNP}_m = G' \frac{k_f}{k_c + k_{NPQ}}, \tag{17}$$

eqn (18) and (19) are obtained for q_{NP}:

$$q_{NP} = \frac{F_m - F'_m}{F_m - F_0} = \frac{k_{NPQ}(k_c + k_p)}{(k_p + k_{NPQ})k_p} \tag{18}$$

$$q_{NP}^{AuNP} = \frac{k_{NPQ}(k_c + k_{ct} + k_p)}{(k_p + k_{NPQ})(k_c + k_p)}. \tag{19}$$

In terms of the rate constants, the inequality (15) is given by eqn (20):

$$\frac{k_{NPQ}(k_c + k_p)}{(k_p + k_{NPQ})k_p} > \frac{k_{NPQ}(k_c + k_{ct} + k_p)}{(k_p + k_{NPQ})(k_{ct} + k_p)}$$
$$\rightarrow \frac{k_c + k_p}{k_p} > \frac{k_c + k_{ct} + k_p}{k_{ct} + k_p} \rightarrow \frac{k_c}{k_p} > \frac{k_c}{k_{ct} + k_p} \tag{20}$$
$$\rightarrow k_p < k_{ct} + k_p \rightarrow k_{ct} > 0.$$

Finally, a lower value for q_{NP}^{AuNP} is the result of the presence of charge transfer to AuNPs and not necessarily to a lower non-photochemical quenching.

This journal is © The Royal Society of Chemistry and Owner Societies 2018

Photochem. Photobiol. Sci., 2018, **17**, 505–516 | **513**

The only photosynthetic parameter whose expression is not affected by k_{ct} is the alternative version of non-photochemical quenching NPQ (eqn (21) and (22)):

$$\text{NPQ} = \frac{F_m - F'_m}{F'_m} = \frac{k_{NPQ}}{k_c} \tag{21}$$

$$\text{NPQ}^{\text{AuNP}} = \frac{k_{NPQ}}{k_c}. \tag{22}$$

In this work, the experimental NPQ slightly decreased in the presence of AuNPs.

Finally for the photochemical quenching the expressions given by eqn (23) and (24) show that k_{ct} is involved in them. However, it is mathematically difficult to establish if the inclusion of k_{ct} would cause a decrease or increase in this parameter.

$$q_P = \frac{F'_m - F_s}{F'_m - F_0} = \frac{\left(\dfrac{k_f}{k_c + k_{NPQ}} - \dfrac{k_f}{k_c + k_{NPQ} + k_p} \right)}{\left(\dfrac{k_f}{k_c + k_{NPQ}} - \dfrac{k_f}{k_c + k_p} \right)} \tag{23}$$

$$= \frac{k_p(k_c + k_p)}{(k_p - k_{NPQ})(k_c + k_{NPQ} + k_p)}$$

$$q_P^{\text{AuNP}} = \frac{\left(\dfrac{k_f}{k_c + k_{NPQ}} - \dfrac{k_f}{k_c + k_{NPQ} + k_{ct} + k_p} \right)}{\left(\dfrac{k_f}{k_c + k_{NPQ}} - \dfrac{k_f}{k_c + k_{ct} + k_p} \right)} \tag{24}$$

$$= \frac{(k_{ct} + k_p)(k_{ct} + k_p + k_c)}{(k_p + k_{ct} - k_{NPQ})(k_c + k_{NPQ} + k_{ct} + k_p)}.$$

DCPIP photoreduction and oxygen evolution

Both the rate of DCPIP photoreduction and the rate of oxygen evolution for chloroplast suspensions increased in the case of inoculation with AuNPs (Fig. 8(a) and (b)).
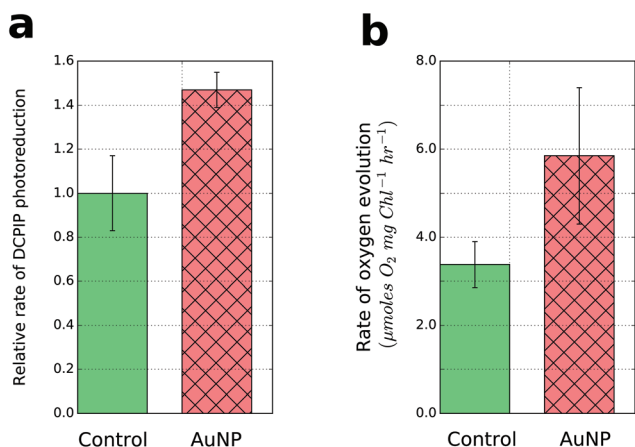

Fig. 8 Measurements of photosynthetic activity of isolated chloroplasts at 20 °C in the presence and absence of AuNPs. (a) The rate of photoreduction of DCPIP by chloroplasts and (b) the rate of evolution of oxygen by chloroplasts under saturating light.

No appreciable reduction of DCPIP was observed in the presence of only AuNPs under either light or dark conditions. This indicates that there was no direct transfer of electrons from the AuNPs to DCPIP. Usually, this probe is used to sense electrons involved in the photosynthetic chain but in our experiments it could also sense the transport of electrons to AuNPs which only occurred in the presence of chloroplasts.

The results obtained for oxygen evolution in the presence of chloroplast and AuNPs can be explained again assuming charge transfer from excited P_{680} to AuNPs took place. This additional charge transfer process augmented P_{680}^+ concentration and consequently increased water splitting with a higher rate of oxygen evolution (Fig. 8b) not necessarily connected with a higher global photosynthetic activity.

Conclusions

The presence of gold nanoparticles highly affected the photophysical properties of both leaves and chloroplasts. The chlorophyll fluorescence was quenched and the emission from PSII was depressed compared to PSI emission.

The Kautsky kinetics was completely altered and almost all the photosynthetic parameters lost their original physical meaning as it was demonstrated by solving the proposed mechanism that included the charge transfer process towards AuNPs. The oxygen evolution and the rate of disappearance of DCPIP were both increased. The results followed the same tendency for intact leaves (after correction for light re-absorption processes) and for chloroplasts. All results were consistent with electron transfer from the excited state of P_{680} to the AuNPs. The apparent increase in the photosynthetic activity observed by indirect methods was not real but was an artificial result caused by the charge transfer processes. This is a crucial point for the evaluation of plant stress caused by certain agents. In this work, in addition to the results about the effect of the AuNPs on the photophysical properties of the plants, it was verified that these stressors that act as electron acceptors from P_{680}^* can falsify measurements of photosynthetic activity based on oxygen evolution Hill reaction and chlorophyll fluorescence.

Conflicts of interest

There are no conflicts to declare.

Acknowledgements

514 | *Photochem. Photobiol. Sci.*, 2018, **17**, 505–516

This journal is © The Royal Society of Chemistry and Owner Societies 2018

References

1 O. V. Salata, *J. Nanobiotechnol.*, 2004, **2**(3), DOI: 10.1186/1477-3155-2-3.

2 D. J. de Aberasturi, A. B. Serrano-Montes and L. M. Liz-Marzán, *Adv. Opt. Mater.*, 2015, **3**, 602–617.

3 M. Li, G. J. Ahammed, C. Li, X. Bao, J. Yu, C. Huang, H. Yin and J. Zhou, *Front. Plant Sci.*, 2016, **7**, 615.

4 P. Lin, S. Lin, P. C. Wang and R. Sridhar, *Biotechnol. Adv.*, 2013, **32**, 711–726.

5 C. J. Murphy, T. K. Sau, A. M. Gole, C. J. Orendorff, J. Gao, L. Gou, S. E. Hunyadi and T. Li, *J. Phys. Chem. B*, 2005, **109**, 13857–13870.

6 C. J. Murphy, A. Gole, S. E. Hunyadi, J. W. Stone, P. N. Sisco, A. Alkilany, B. E. Kinard and P. Hankins, *Chem. Commun.*, 2008, **5**, 544–557.

7 K. L. Kelly, E. Coronado, L. L. Zhao and G. C. Schatz, *J. Phys. Chem. B*, 2003, **107**, 668–677.

8 M. A. El-Sayed, *Acc. Chem. Res.*, 2001, **34**, 257–264.

9 R. Shukla, V. Bansal, M. Chaudhary, A. Basu, R. R. Bhonde and M. Sastry, *Langmuir*, 2005, **21**, 10644–10654.

10 V. L. Colvin, *Nat. Biotechnol.*, 2003, **23**, 1166–1170.

11 O. A. Sadik, A. L. Zhou, S. Kikandi, N. Du, Q. Wang and K. Varner, *J. Environ. Monit.*, 2009, **11**, 1782–1800.

12 J. Boken, P. Khurana, S. Thatai, D. Kumar and S. Prasad, *Appl. Spectrosc. Rev.*, 2017, **52**, 774–820.

13 E. Corredor, P. S. Testillano, M. J. Coronado, P. González-Melendi, R. Fernández-Pacheco, C. Marquina, M. R. Ibarra, J. M. De La Fuente, D. Rubiales, A. Pérez-De-Luque and M. C. Risueño, *BMC Plant Biol.*, 2009, **9**, 45.

14 T. Eichert, A. Kurtz, U. Steiner and H. E. Goldbach, *Physiol. Plant.*, 2008, **134**, 151–160.

15 C. Buschmann, *Photosynth. Res.*, 2007, **92**, 261–271.

16 I. Moya and Z. G. Cerovic, Remote sensing of chlorophyll fluorescence: instrumentation and analysis, in *Chlorophyll a Fluorescence. Advances in Photosynthesis and Respiration*, ed. G. C. Papageorgiou and Govindjee, Springer, Dordrecht, NLD, 2004, pp. 429–445.

17 K. Maxwell and G. N. Johnson, *J. Exp. Bot.*, 2000, **51**, 659–668.

18 M. Lang, F. Stober and H. K. Lichtenthaler, *Radiat. Environ. Biophys.*, 1991, **30**, 333–347.

19 E. Pfündel, *Photosynth. Res.*, 1998, **56**, 185–195.

20 F. Franck, P. Juneau and R. Popovic, *Biochim. Biophys. Acta, Bioenerg.*, 2002, **1556**, 239–246.

21 G. B. Cordon and M. G. Lagorio, *Photochem. Photobiol. Sci.*, 2006, **5**, 735–740.

22 H. K. Lichtenthaler, C. Buschmann and M. Knapp, *Photosynthetica*, 2005, **43**, 379–393.

23 S. Barazzouk, P. V. Kamat and S. Hotchandani, *J. Phys. Chem. B*, 2005, **109**, 716–723.

24 S. Barazzouk, L. Bekalé and S. Hotchandani, *J. Mater. Chem.*, 2012, **22**, 25316.

25 W. F. Falco, E. R. Botero, E. A. Falcão, E. F. Santiago, V. S. Bagnato and A. R. L. Caires, *J. Photochem. Photobiol., A*, 2011, **225**, 65–71.

26 J. P. Giraldo, M. P. Landry, S. M. Faltermeier, T. P. McNicholas, N. M. Iverson, A. A. Boghossian, N. F. Reuel, A. J. Hilmer, F. Sen, J. A. Brew and M. S. Strano, *Nat. Mater.*, 2014, **13**, 400–408.

27 J. W. Slot and H. J. Geuze, *Eur. J. Cell Biol.*, 1985, **38**, 87–93.

28 D. Joly and R. Carpentier, Rapid Isolation of Intact Chloroplasts from Spinach Leaves, in *Photosynthesis Research Protocols. Methods in Molecular Biology*, ed. R. Carpentier, Humana Press, Totowa NJ, 2011, pp. 321–325.

29 R. L. Dean and E. Miskiewicz, *Mol. Biol. Educ.*, 2003, **31**, 410–417.

30 M. E. Ramos and M. G. Lagorio, *Photochem. Photobiol. Sci.*, 2004, **3**, 1063–1066.

31 A. Iriel, G. Dundas, A. Fernández Cirelli and M. G. Lagorio, *Chemosphere*, 2014, **119C**, 697–703.

32 J. M. Novo, A. Iriel and M. G. Lagorio, *Photochem. Photobiol. Sci.*, 2012, **11**, 724.

33 A. Ventrella, L. Catucci and A. Agostiano, *Bioelectrochemistry*, 2010, **79**, 43–49.

34 D. A. Walker, *Photosynth. Res.*, 2002, **73**, 51–54.

35 T. Delieu and D. A. Walker, *New Phytol.*, 1972, **71**, 201–225.

36 D. Joly, S. Govindachary and M. Fragata, Photosystem II Reconstitution into Proteoliposomes and Methodologies for Structure–Function Characterization, in *Photosynthesis Research Protocols. Methods in Molecular Biology*, ed. R. Carpentier Humana Press, Totowa NJ, 2011, pp. 217–245.

37 D. A. Sims and J. A. Gamon, *Remote Sens. Environ.*, 2002, **81**, 337–354.

38 R. J. Porra, W. A. Thompson and P. E. Kriedemann, *Biochim. Biophys. Acta, Bioenerg.*, 1989, **975**, 384–394.

39 H. Barabadi, S. Honary, P. Ebrahimi, M. A. Mohammadi, A. Alizadeh and F. Naghibi, *Braz. J. Microbiol.*, 2014, **45**, 1493–1501.

40 A. Wang, H. P. Ng, Y. Xu, Y. Li, Y. Zheng, J. Yu, F. Han, F. Peng and L. Fu, *J. Nanomater.*, 2014, 451232.

41 A. Habib, M. Tabata and Y. G. Wu, *Bull. Chem. Soc. Jpn.*, 2005, **78**, 262–269.

42 W. Haiss, N. T. K. Thanh, J. Aveyard and D. G. Fernig, *Anal. Chem.*, 2007, **79**, 4215–4221.

43 V. Amendola and M. Meneghetti, *J. Phys. Chem. C*, 2009, **113**, 4277–4285.

44 J. Zhou, D. A. Beattie, J. Ralston and R. Sedev, *Langmuir*, 2007, **23**, 12096–12103.

45 L. V. Natarajan, J. E. Ricker, R. E. Blankenship and R. Chang, *Photochem. Photobiol.*, 1984, **39**, 301–306.

46 S. Rajagopal, E. A. Egorova, N. G. Bukhov and R. Carpentier, *Biochim. Biophys. Acta, Bioenerg.*, 2003, **1606**, 147–152.

47 G. Beddard, G. Porter and G. Weese, *Proc. R. Soc. London, Ser. A*, 1975, **342**, 317–325.

This journal is © The Royal Society of Chemistry and Owner Societies 2018

Photochem. Photobiol. Sci., 2018, **17**, 505–516 | **515**

48 V. D. Samuilov, A. Yu. Borisov, E. L. Barsky, O. F. Borisova and A. V. Kitashov, *IUBMB Life*, 1998, **46**, 333–341.

49 J. W. Lee, W. Zipfel and T. G. Owens, *J. Lumin.*, 1992, **51**, 79–89.

50 Y. Kato, M. Sugiura, A. Oda and T. Watanabe, *Proc. Natl. Acad. Sci. U. S. A.*, 2009, **106**, 17365–17370.

51 S. Merchant and M. R. Sawaya, *Plant Cell*, 2005, **17**, 648–663.

52 M. D. Scanlon, P. Peljo, M. A. Méndez, E. Smirnov and H. H. Girault, *Chem. Sci.*, 2015, **6**, 2705–2720.

53 L. Hendrickson, R. T. Furbank and W. S. Chow, *Photosynth. Res.*, 2004, **82**, 73–81.